LBL-12255
Preprint c.2

Lawrence Berkeley Laboratory
UNIVERSITY OF CALIFORNIA

Accelerator & Fusion
Research Division

RECEIVED
JUN 2 1981
DOCUMENTS

Submitted to the Review of Scientific Instruments

EFFECT OF A MAGNETIC FILTER ON HYDROGEN ION SPECIES IN A MULTICUSP ION SOURCE

K.W. Ehlers and K.N. Leung

March 1981

TWO-WEEK LOAN COPY

This is a Library Circulating Copy
which may be borrowed for two weeks.
For a personal retention copy, call
Tech. Info. Division, Ext. 6782

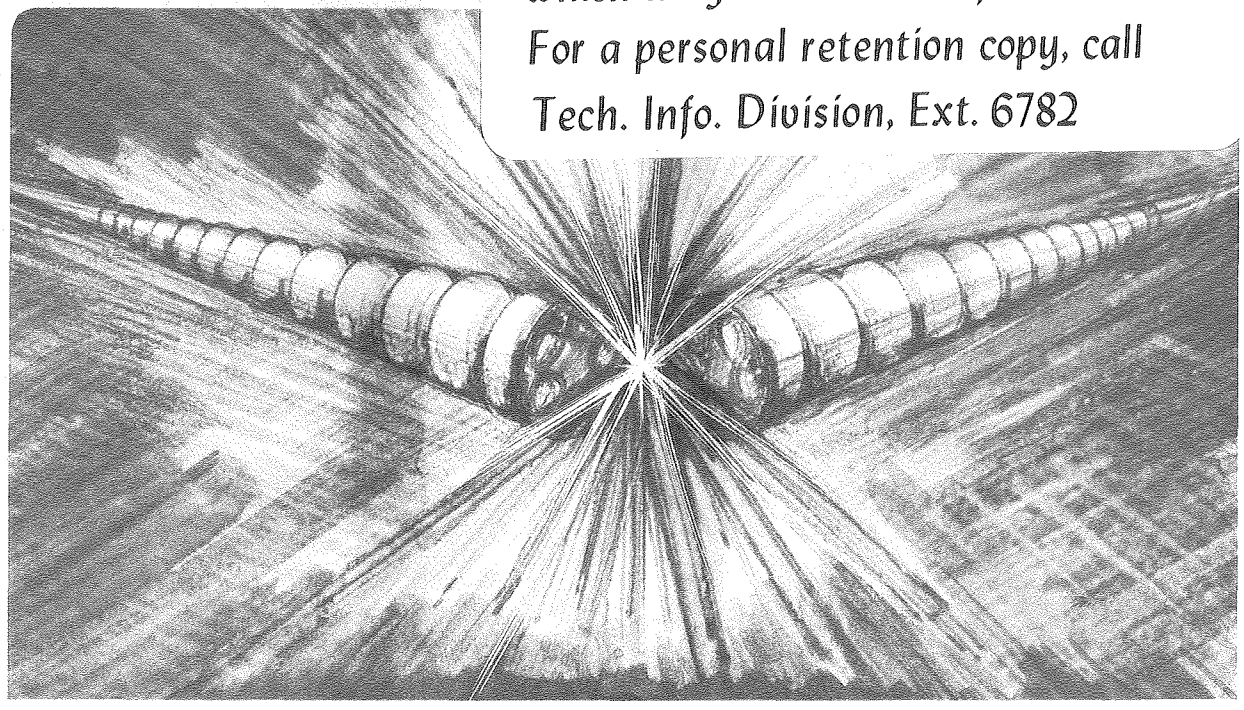

Prepared for the U.S. Department of Energy under Contract W-7405-ENG-48

LBL-12255
c.2

DISCLAIMER

This document was prepared as an account of work sponsored by the United States Government. While this document is believed to contain correct information, neither the United States Government nor any agency thereof, nor the Regents of the University of California, nor any of their employees, makes any warranty, express or implied, or assumes any legal responsibility for the accuracy, completeness, or usefulness of any information, apparatus, product, or process disclosed, or represents that its use would not infringe privately owned rights. Reference herein to any specific commercial product, process, or service by its trade name, trademark, manufacturer, or otherwise, does not necessarily constitute or imply its endorsement, recommendation, or favoring by the United States Government or any agency thereof, or the Regents of the University of California. The views and opinions of authors expressed herein do not necessarily state or reflect those of the United States Government or any agency thereof or the Regents of the University of California.

Effect of a Magnetic Filter on Hydrogen Ion Species in a Multicusp Ion Source

K. W. Ehlers and K. N. Leung

Lawrence Berkeley Laboratory
University of California
Berkeley, California 94720

Abstract

Hydrogen ion species and discharge characteristics have been compared for two different magnet geometries in a multicusp ion source. One magnet configuration indicated that the H_2^+ ion percentage in the extracted beam could be reduced by eliminating the high energy ionizing electrons near the ion extraction region. To accomplish this and maintain the desire features of both magnet geometries, a magnetic filter was installed near the source exit. With this combined arrangement, we found that the H^+ ion percentage and discharge condition were much improved and a more uniform profile across the extraction plane was achieved. The atomic species fraction can then be further enhanced by the addition of low energy ($\sim$16 eV) primary electrons into the source plasma chamber.

Introduction

Multicusp plasma devices are capable of producing large volumes of uniform and quiescent plasma with densities exceeding 10^{12} ions/c.c.[1,2] Recently, there has been a growing interest in applying such devices as ion sources for neutral beam injection systems[3-6] and for particle accelerators.[7,8]

To increase plasma penetration by a neutral beam, a high percentage of H^+ or D^+ is desired. Thus we have investigated the hydrogen ion species composition in a multicusp source with two different magnet configurations. The results of this investigation indicated that the presence of primary ionizing electrons in the vicinity of the ion extraction grid increased the percentage of the H_2^+ ions in the extracted beam. To take advantage of this observation, a permanent magnet filter was installed across the source chamber to eliminate the presence of these ionizing electrons in the front region of the source. The use of this filter with the longitudinal cusp geometry greatly improved the atomic species as well as the source operability and the plasma density profile. It is also possible to further enhance the H^+ ion percentage in this arrangement by injecting 16 eV electrons from a second set of cathodes into the source plasma. These electrons cannot produce H_2^+ ions, but they can dissociate the hygrogen gas molecules and the molecular ion species.

I. Experimental Apparatus

The experiment was performed in a 20 cm diam by 30 cm long stainless steel chamber with the open end enclosed by a three-grid extraction system. Samarium-cobalt magnets ($B_{max} \approx 3.6$ kG) can be mounted easily on the external

surface of the source chamber to generate continuous line-cusp configurations which are used for primary electron and plasma confinement.[2] A schematic diagram of the ion source is shown in Fig. 1. A steady-state hydrogen plasma was produced by primary ionizing electrons emitted from six, 0.05-cm-diam tungsten filaments, which were biased at approximately -70 V, with respect to the source chamber wall which served as the anode.

The ion beam was extracted by means of a standard Berkeley accel-decel three electrode system with the first multi-slot plasma grid masked down to an extraction aperture of about 2 cm diameter. The source was operated with the plasma grid either floating or connected to the source chamber, which in turn was biased at a positive ion extraction potential ($\sim$ 300 V) relative to ground. The outermost grid was electrically grounded and the center grid was biased at -60 V so as to retard any back-streaming electrons. A compact magnetic-deflection mass spectrometer[9] was installed just outside the extractor to measure the hydrogen ion species distribution of the extracted beam. In normal operation, the pressure indicated by an ionization gauge located downstream from the mass spectrometer was about 1×10^{-4} Torr. This pressure is sufficiently low that dissociation and charge-exchange processes are minimized in the region between the extractor and the spectrometer. The actual source pressure was approximately 1.5×10^{-3} Torr. Plasma parameters and saturated ion current density profiles were obtained by using movable Langmuir probes.

II. Magnet Configurations

Plasma confinement by different magnet geometries has been studied by Leung et al.[2] It is found that the continuous line-cusp configuration is more efficient than the broken cusps or the checkerboard arrangement. When operated

as an ion source, continuous line-cusps can be formed either by mounting columns of magnets parallel (longitudinal) to the source axis (Fig. 1(b)) or by installing rings of magnets around the chamber perpendicular to the source axis (Fig. 1(a)). Since the magnets are external, the two line-cusp configurations could be interchanged easily without opening the vacuum system.

(a) Longitudinal

With the magnets arranged to form longitudinal line-cusps (Fig. 1(b)), the plasma density profile in front of the plasma grid (Fig. 2) had a uniform region of about 6 cm diam. The fact that the plasma grid was floating at $\sim$40 V below the anode potential, together with the complete Langmuir probe characteristics of Fig. 3(a), indicate that a sizeable number of high energy electrons are present near the ion extraction region. These electrons can cause ionization in front of the plasma grid. As a result, a high percentage of H_2^+ ions will be contained in the extracted beam and this is illustrated by the spectrometer output signal in Fig. 4(a).

Figure 5 shows the ion species distribution as a function of discharge current I_d. For $I_d < 15$ A, the percentage of H_2^+ in the beam is greater than 40%. The atomic species H^+ increases with I_d, reaching about 40% at $I_d \approx 15$ A. The source became quite unstable when $I_d \approx 20$ A, and attempts to increase I_d by increasing the filament heating current ended up with the filaments being destroyed. Whether this instability was a "mode" change[5] was not determined, however satisfactory operation in excess of $I_d \approx 20$ A with this test geometry was not possible.

(b) Rings

When the magnets were arranged in rings around the chamber (Fig. 1(a)), the source could be operated satisfactorily with a high discharge current

and at the same gas pressure as the longitudinal cusp configuration. The H_2^+ fraction in the beam was found to be much smaller as illustrated by the spectrometer signal in Fig. 4(b). In fact, for $I_d < 30$ A, Fig. 6 shows that the percentage of H_2^+ ions is less than 8%, while the percentage of the H^+ ions increases from 32 to 76% as I_d is varied from 5 to 30 A. Thus, this ring cusp geometry yielded a much larger fraction of H^+ ions than the longitudinal cusp configuration. The big increase in atomic species of this magnet geometry is attributed to the filtering effect of primary ionizing electrons by the radial component of the B-field in the successive magnetic wells as illustrated in Fig. 1(a). The Langmuir probe traces obtained near the center of the plasma grid (Fig. 3(b)) demonstrate that only very low energy electrons are present in the front part of the source. Therefore, the production of H_2^+ ions by energetic electrons near the extraction grid is much reduced. However, this test ring-cusp geometry produces no radial B-field at the axis of the source chamber. Instead, an alternating axial B-field of approximately 50 G is present in that region. Thus primary ionizing electrons can still tunnel through to the extraction region along the axis, resulting in a poor density profile at the extraction plane which is sharply peaked at the center as shown in Fig. 7(a).

Figure 7(b) shows that the floating potential V_f, measured by the movable Langmuir probe in front of the plasma grid, follows the shape of the density profile. This indicates that the number of energetic electrons varies with the radial position and thus it is suspected that the species distribution will also vary accordingly. In this experiment, the entrance slit of the spectrometer was located about 1.5 cm from the center and the floating potential there was more positive than that of the center position. As the diameter of the source chamber is increased, the magnitude of the filtering B-field will

br reduced. Hence, the density profile for the ring geometry would improve.[10] At the same time, the atomic species fraction in the beam is expected to decrease due to the reduction in the radial component of the B-field which in turn allows the energetic electrons to reach the grid region.

III. Permanent Magnet Filter

To take advantage of the results obtained from the ring-cusp geometry, a permanent magnet "filter" which provided a limited region of transverse B-field to confine energetic electrons was installed across the front part of the source chamber (Fig. 1(c)). This filter was used along with the Longitudinal-cusp configuration as it was this magnet geometry that produced the desired plasma density profile. The magnets were enclosed in water-cooled channels and they were arranged with opposite polarity facing each other as shown in Fig. 8.[11] The magnitude of the B-field was adjusted by employing ceramic bar-magnets with different thicknesses.

With the filter in position, the source is essentially divided into two chambers. One chamber, which is a complete multicusp plasma source with one leaky side, contains the energetic electrons and is therefore the ion source chamber where all the ionization occurs. The other chamber, which is the ion extraction region, contains a plasma with only low energy electrons. If the B-field of the filter is made only strong enough to return the primary electrons to the source chamber, positive ions as well as cold electrons can still diffuse into the ion extraction chamber.[12] The exact process of how the low energy electrons are allowed to escape across the B-field is not yet fully understood, however, it may be recognized as the same effect which we encountered in our study of the plasma in the exit region of the self-

extraction negative ion source.[13,14] With only low energy electrons present in the ion extraction chamber, very few H_2^+ ions are formed in this region.

With the addition of the filter, the source has been operated continuously with a discharge current as high as 90 A (limited by the power supply) without the previous indicated instability. The plasma density in the extraction chamber is always less than that in the source chamber, and this reduction is a function of the magnitude and thickness of the filter magnetic field, as well as to the filter's geometric transparency. With a strong B-field, this reduction can be as high as two orders of magnitude.[13,14] The filter has been tested with three values of B-field; namely 25, 40, and 65 G with thickness of about 3 cm. As the field strength of the filter is increased from 25 to 65 G, the H^+ ion species percentage increases from about 60 to 78% with I_d = 80 A, but the ion current density in the extraction plane decreases (Fig. 9). With a 40-gauss-filter, Fig. 10 shows that the plasma density profile in front of the plasma grid has a uniform region of approximately 7 cm diam which is slightly larger than the case without the filter.

The ion extraction chamber can be isolated electrically from the source chamber as illustrated in Fig. 1(c). By biasing the plasma grid together with the extraction chamber several volts negative with respect to the source chamber, the ion current density at the extraction plane is increased by approximately 30% as shown in Fig. 11. This increase in ion current density is accompanied by an increase in the electron temperature as shown in Fig. 12. At the same time, the plasma potential near the grids, as indicated by the knee of the probe trace, also becomes more positive with respect to the wall of the extraction chamber. However, the plasma potential in the source chamber remains at +4 volts relative to the source chamber wall. Thus, the potential of the plasma in the extraction chamber is approximately 2 volts more negative

than that of the source chamber for all bias voltages.

To improve the geometric transparency, a new filter has been constructed by installing thin ceramic magnet rods (cross-sectional area = 3.5 x 3.5 mm^2) into six 0.6 cm diam copper tubings that are placed 4 cm apart. In this arrangement, the magnets are well cooled by running water through the spacing between the magnets and the tubing-wall. Figure 13 shows the B-field variation across this filter. When the source was operated with I_d = 10 A, the total ion current collected by the plasma grid in the presence of the filter was 1.22 A which corresponds to a current density of about 10 mA/cm^2. Without the filter, the total ion current collected was 1.8 A for the same discharge current. Therefore the effective transparency of this filter is approximately 68%. Figure 14 shows the variation of species composition as a function of discharge current. In general, the H^+ ion fraction is about six percentage points higher than the case without the filter for the same discharge current (for $I_d < 30$ A). Optimization of the B-field and magnet geometry of the filter is in progress and results will be reported. A large scale experiment has also been planned to test the effectiveness of this type of filter at high density pulsed operation.

IV. Low Energy Electron Injection

In the presence of the filter, the source has been operated with I_d as hgih as 90 A. In order to further enhance the H^+ ion percentage, primary electrons with energy approximately equal to 16 eV were injected into the source chamber from a second set of cathodes. The high density in this chamber is particularly favorable for the space-charge-limited emission of these low energy electrons. Once inside the source plasma, these electrons cannot produce H_2^+ (the threshold energy for ionizing H_2 is 15.8 eV), but they can dissociate the hydrogen gas molecules [15] and the molecular ion species H_2^+ and

H_3^+. Figure 15 shows that for the 40-gauss-filter and with I_d = 90 A, the atomic species percentage is increased from 72 to 81% by the addition of 40 A of 16 eV electrons. With a 65-gauss-filter and I_d = 90 A, the addition of 50 A of 16 eV electrons increases the H^+ ion composition to about 90%. No significant change in the ion current density at the extraction plane has been observed with the addition of these 16 eV electrons. Thus, this technique can be of interest after one has obtained the desired extraction ion current density at the grid and wishes to increase the atomic component without changing the ion density.

Acknowledgments

We would like to thank H. Tolleth for all the technical assistance and members of the LBL neutral beam group for valuable discussions. The skillful technical work of L.A. Biagi, H.H. Hughes and members of their group is also gratefully acknowledged. This work is supported by the Director, Office of Fusion Energy, Development & Technology Division, of the U.S. Department of Energy under Contract No. W-7405-ENG-48.

References

1. R. Limpaecher and K. R. MacKenzie, Rev. Sci. Instrum. 44, 726 (1973).
2. K. N. Leung, T. K. Samec, and A. Lamm, Phys. Lett. A51, 490 (1975).
3. Plasma Physics and Fusion Progress Report, Culham Lab. Rep. CLM-PR 20, 1978.
4. W. L. Stirling, P. M. Ryan, C. C. Tsai, and K. N. Leung, Rev. Sci. Instrum. 50, 102 (1979).
5. K. W. Ehlers and K. N. Leung, Rev. Sci. Instrum. 50, 1353 (1979).
6. Japan Atomic Energy Research Institute Report JAERI-M 8869 (1980).
7. J. Grando, H. Haseroth, C. Hill, M. Hone, Proc. 1979 Linear Acc. Conf., Brookhaven, BNL-51134.
8. R. Keller and N. Angert, Pro. 1979 Linear Acc. Conf., Brookhaven, BNL-51134.
9. K. W. Ehlers, K. N. Leung, and M. D. Williams, Rev. Sci. Instrum., 50, 1031 (1979).
10. A. P. H. Goede and T. S. Green, 1979 8th Symp. on Engineering Problems of Fusion Research, San Francisco IEEE 79 CH1441-5NPS.
11. K. N. Leung, G. R. Taylor, J. M. Barrick, S. L. Paul and R. E. Kribel, Phys. Lett. A57, 145 (1976).
12. K. N. Leung, Proceedings of the Symp. on Production and Neutralization of Negative Hydrogen Ions and Beams (Brookhaven Nat. Lab., Sept. 1977).
13. K. W. Ehlers and K. N. Leung, Rev. Sci. Instrum. 51, 721 (1980).
14. K. W. Ehlers and K. N. Leung, Appl. Phys. Lett. 38, 287 (1981).
15. C. F. Barnett et. al., "Atomic Data for Controlled Fusion Research," ORNL-5207, p.C.3.2 (1977).

Figure Captions

Fig. 1 Schematic diagram of the ion source showing (a) the ring-cusp, (b) the longitudinal line-cusp, and (c) the longitudinal line-cusp with the magnetic filter.

Fig. 2 The radial density profile near the plasma grid for the longitudinal line-cusp geometry.

Fig. 3 Langmuir probe traces obtained near the plasma grid for (a) the longitudinal line-cusp, and (b) the ring-cusp geometry.

Fig. 4 The spectrometer output signal showing the hydrogen species for (a) the longitudinal line-cusp, and (b) the ring-cusp geometry at the same neutral gas pressure.

Fig. 5 The hydrogen ion species distribution as a function of discharge current for the longitudinal line-cusp geometry.

Fig. 6 The hydrogen ion species distribution as a function of discharge current for the ring-cusp geometry.

Fig. 7 (a) The density profile and (b) the floating potential as a function of radial position near the plasma grid for the ring-cusp geometry.

Fig. 8 The permanent magnet filter.

Fig. 9 (a) The ion saturation current obtained by a Langmuir probe near the plasma grid, and (b) the hydrogen ion species distribution as a function of the filter magnetic field.

Fig. 10 The radial density profile near the plasma grid for the longitudinal line-cisp geometry with the magnetic filter.

Fig. 11 Ion saturation current obtained by a Langmuir probe near the plasma grid as a function of the bias voltage between the source chamber and the plasma grid together with the extraction chamber.

Fig. 12 Langmuir probe characteristics obtained near the plasma grid for different bias voltages between the source chamber and the plasma grid together with the extraction chamber. The zero reference potential is the potential of the extraction chamber wall.

Fig. 13 A plot of the magnetic field across the plane of the filter in between two magnet rods.

Fig. 14 Hydrogen ion species distribution as a function of discharge current for the case with (solid lines) and without (dotted lines) the filter.

Fig. 15 The spectrometer output signal showing the hydrogen ion species for the case (a) without and, (b) with the addition of 16 eV electrons.

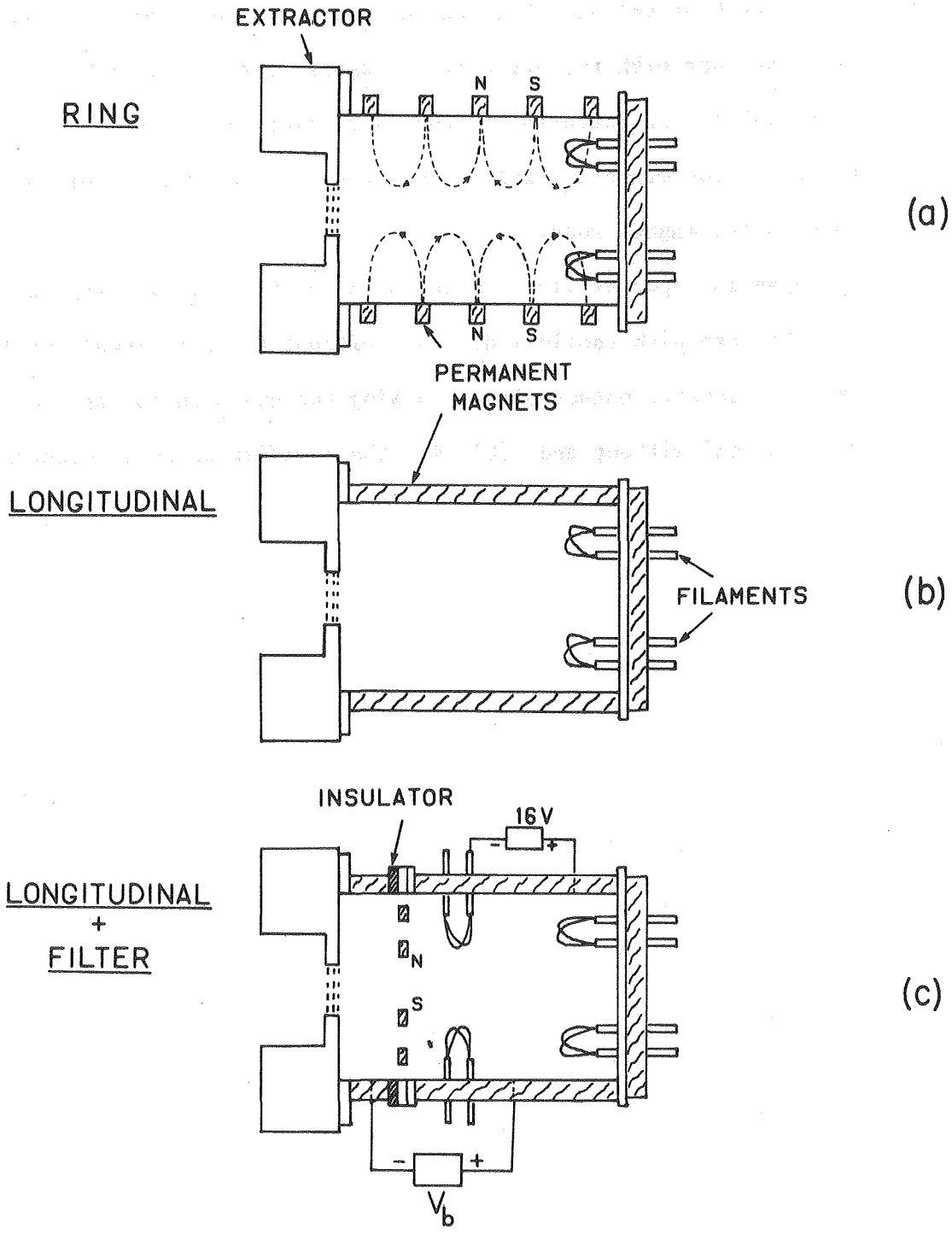
EXTRACTOR
RING
N
S
N
S
PERMANENT
MAGNETS
(a)
LONGITUDINAL
FILAMENTS
(b)
INSULATOR
16V
LONGITUDINAL
+
FILTER
N
S
V_b
(c)
XBL 813-8747A

Fig. 1

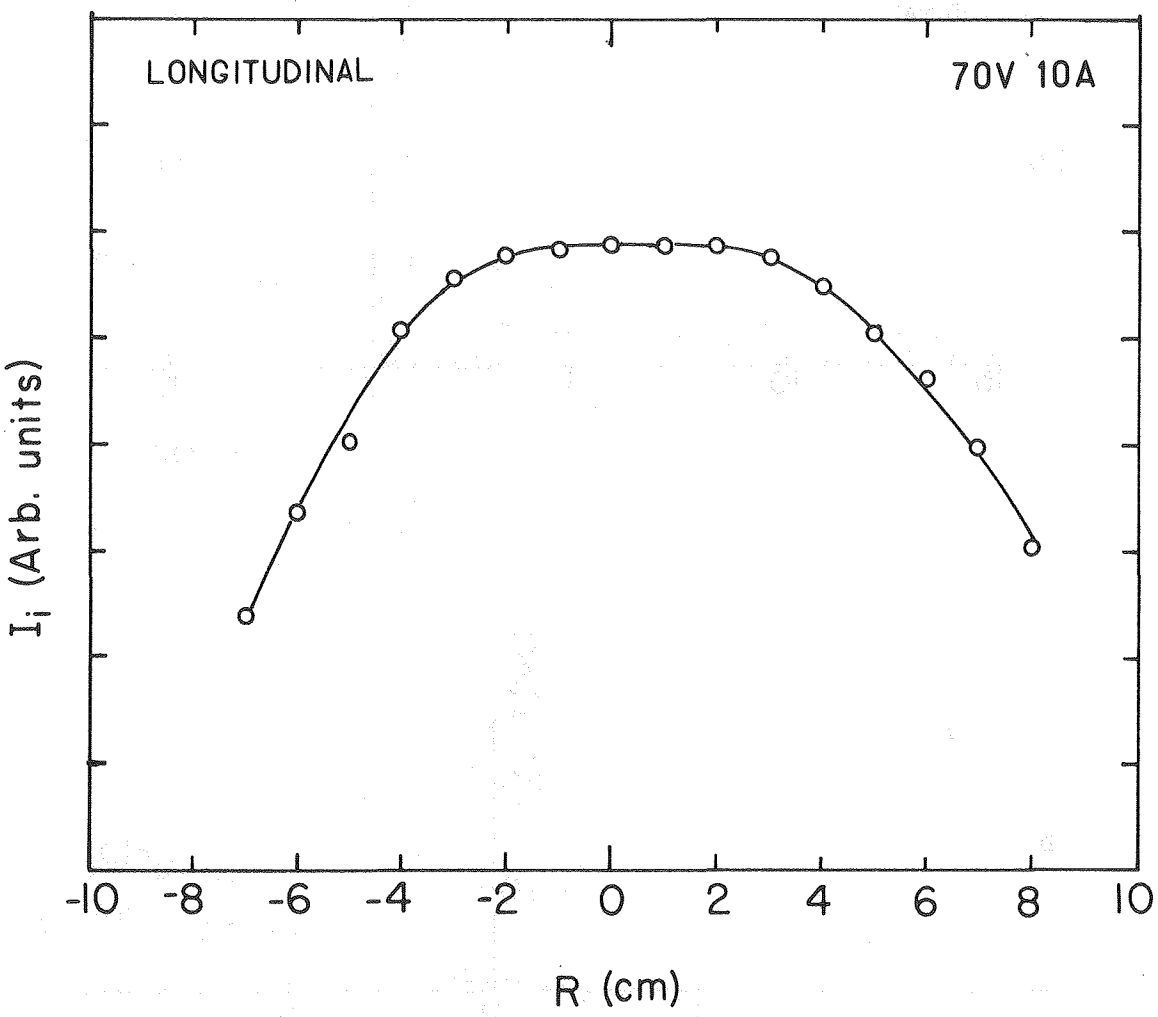

XBL 813-8743

Fig. 2

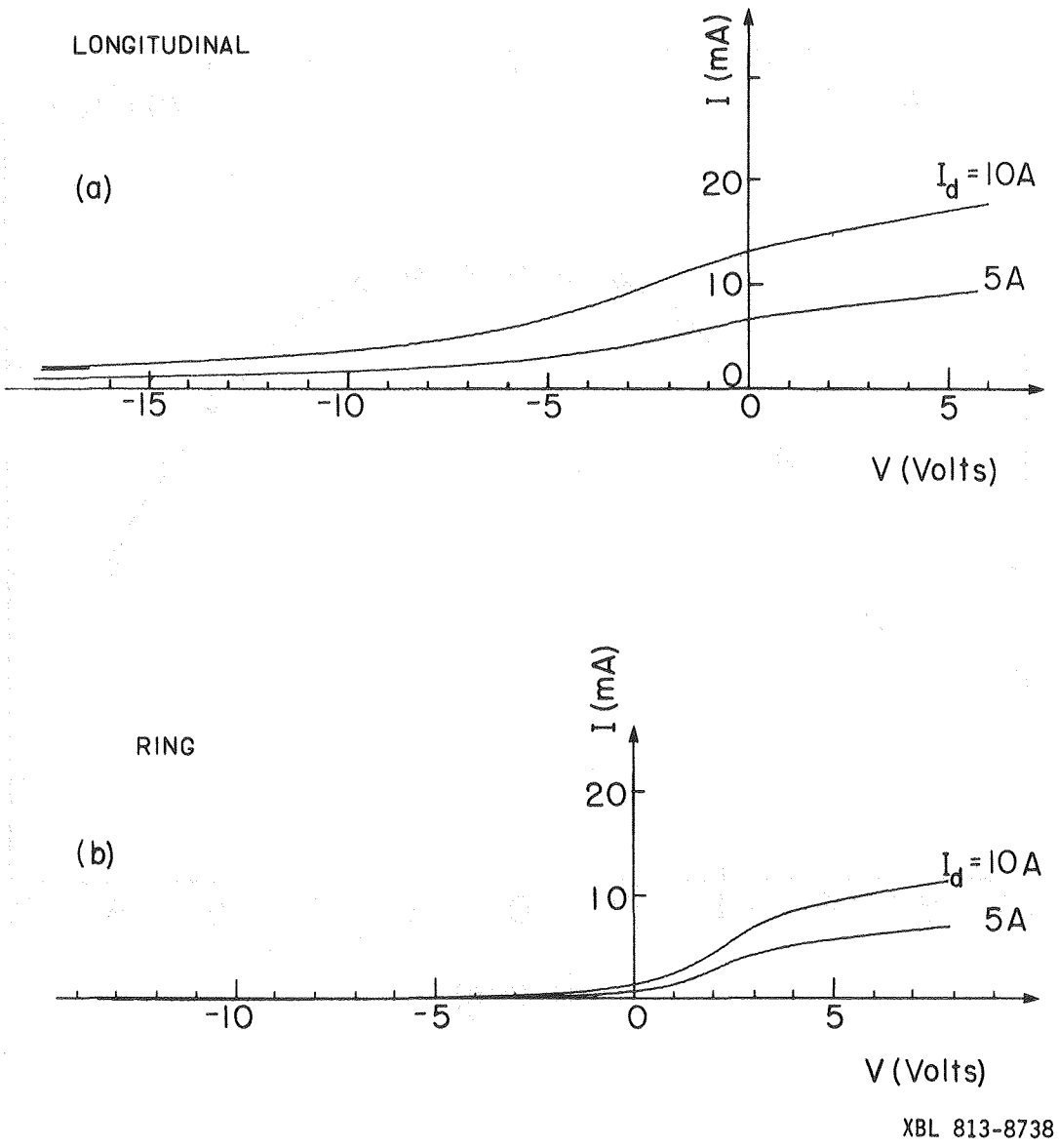
LONGITUDINAL
(a)
I (mA)
20
10
0
I_d = 10A
5A
-15
-10
-5
0
5
V (Volts)
RING
(b)
I (mA)
20
10
I_d = 10A
5A
-10
-5
0
5
V (Volts)
XBL 813-8738

Fig. 3

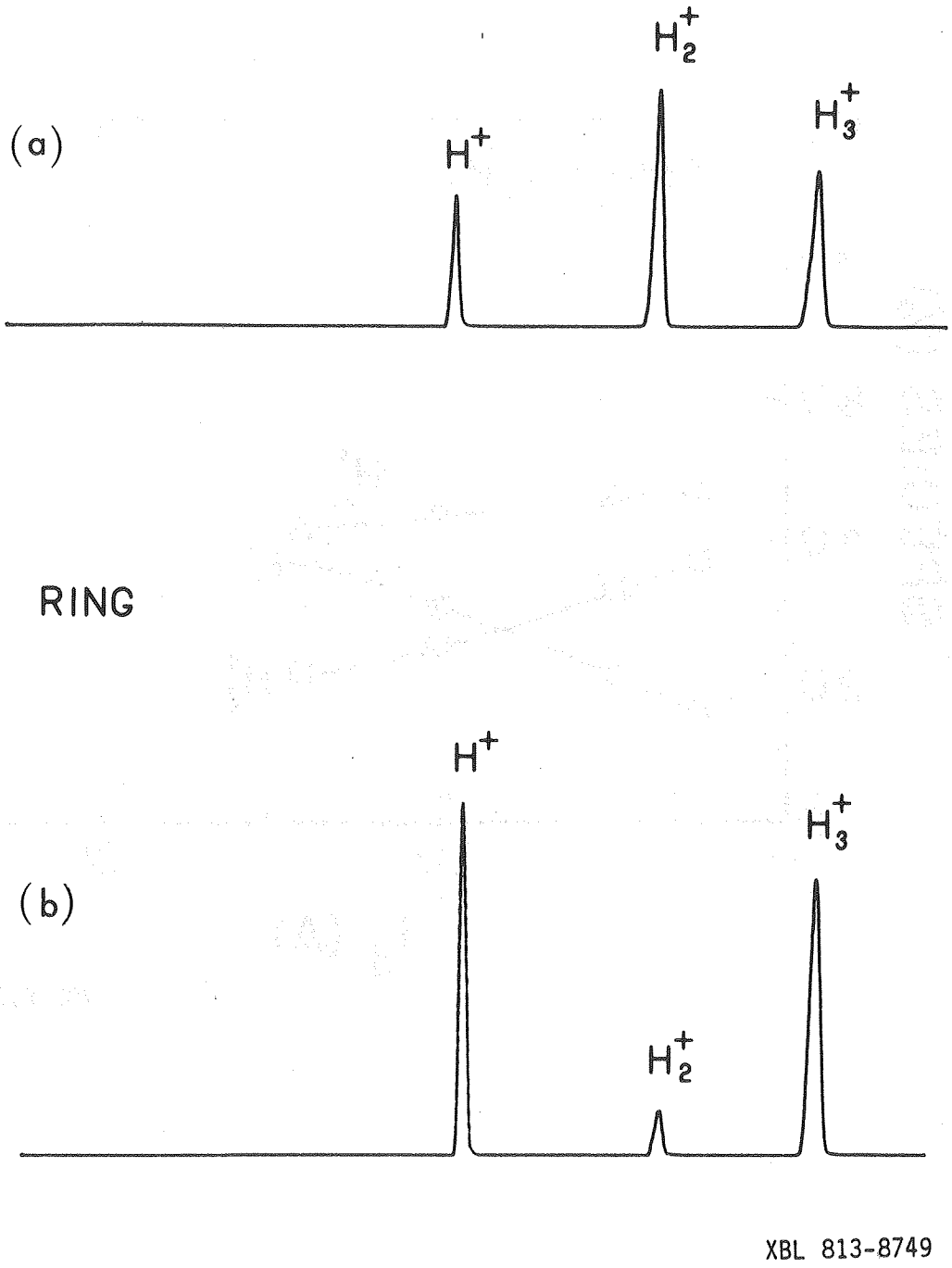

Fig. 4

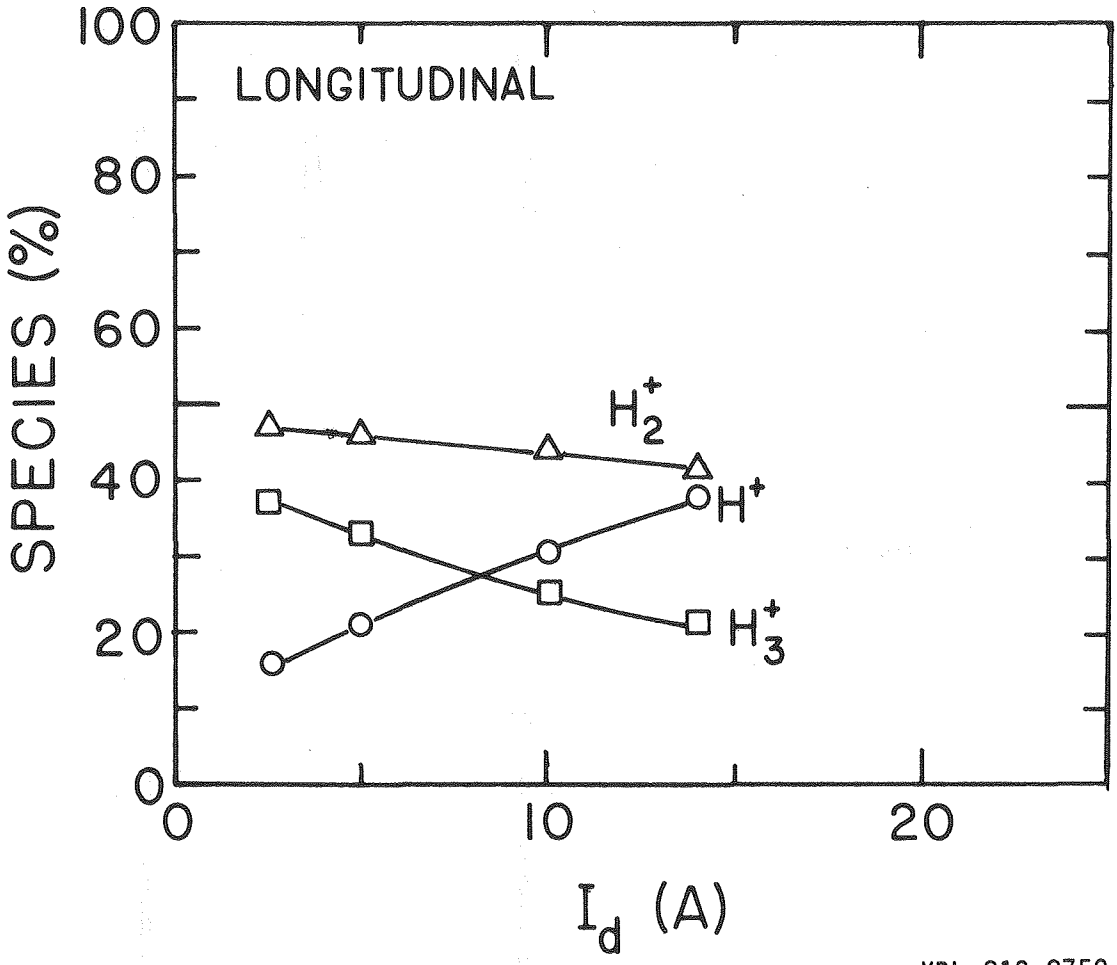
LONGITUDINAL
SPECIES (%)
100
80
60
40
20
0
0
10
20
I_d (A)
H_2^+
H^+
H_3^+
XBL 813-8750

Fig. 5

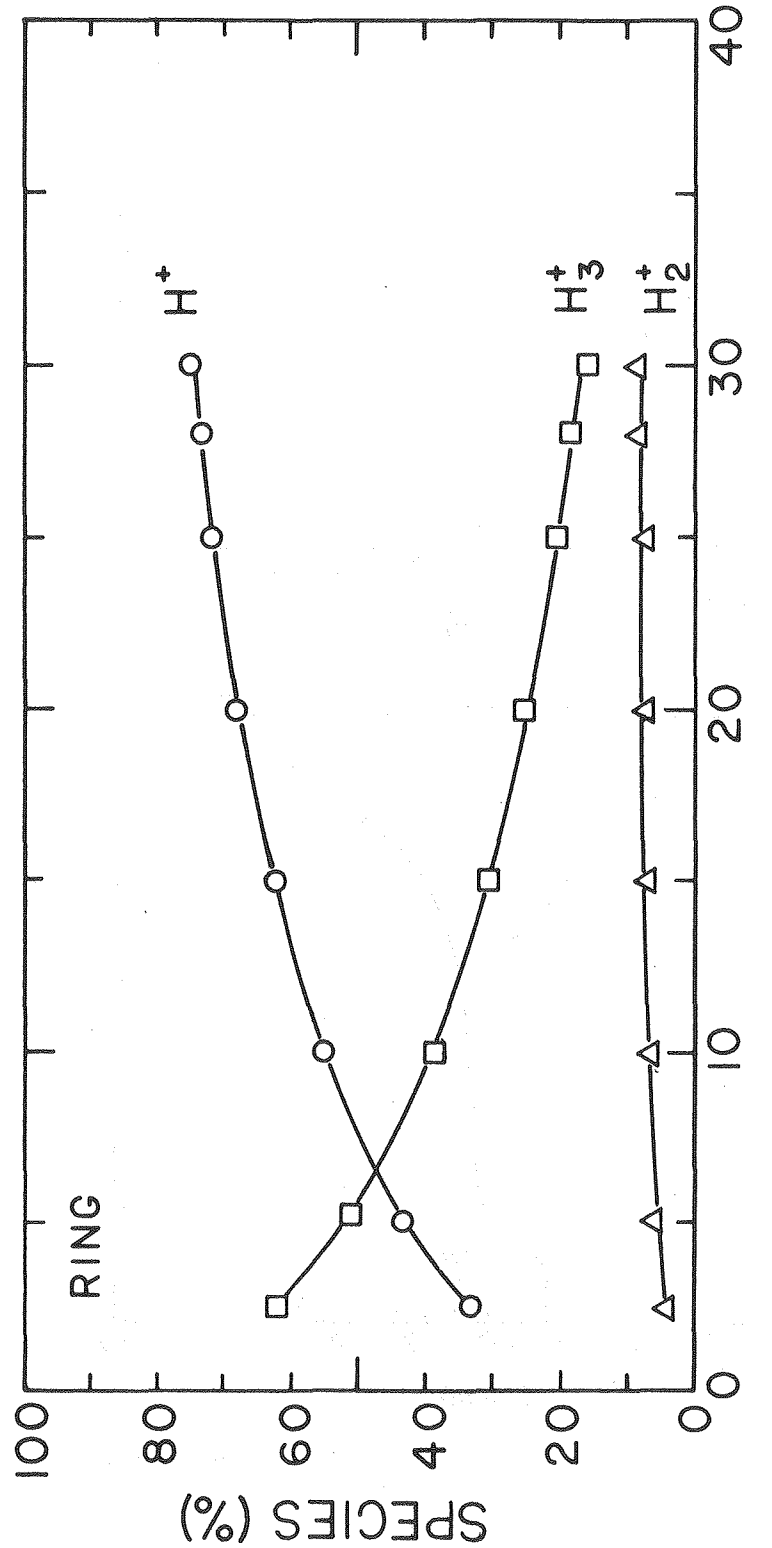

XBL 813-8741

Fig. 6

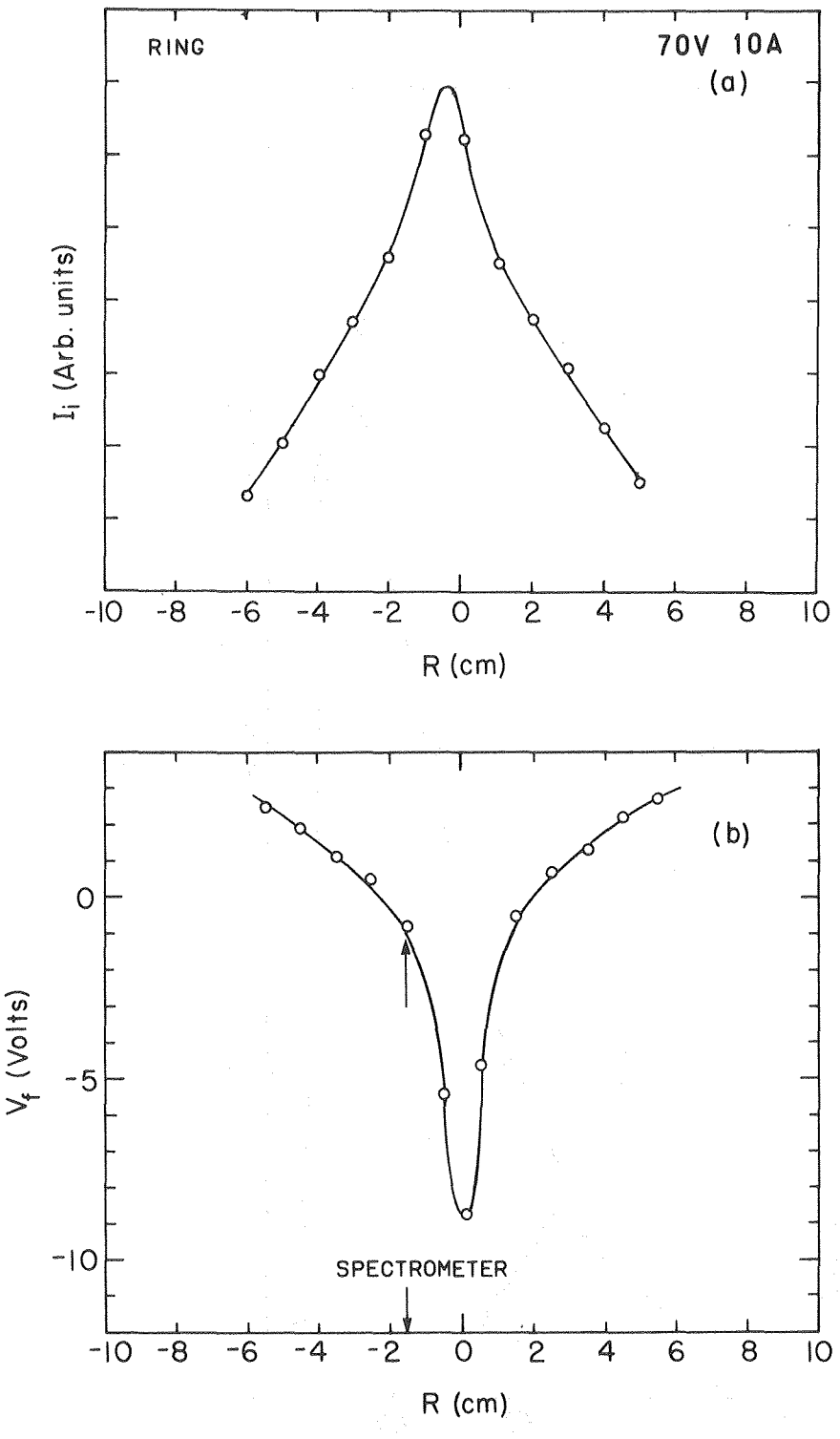
RING
70V 10A
(a)
I_i (Arb. units)
-10 -8 -6 -4 -2 0 2 4 6 8 10
R (cm)
(b)
V_f (Volts)
0
-5
-10
SPECTROMETER
-10 -8 -6 -4 -2 0 2 4 6 8 10
R (cm)
XBL 813-8739

Fig. 7

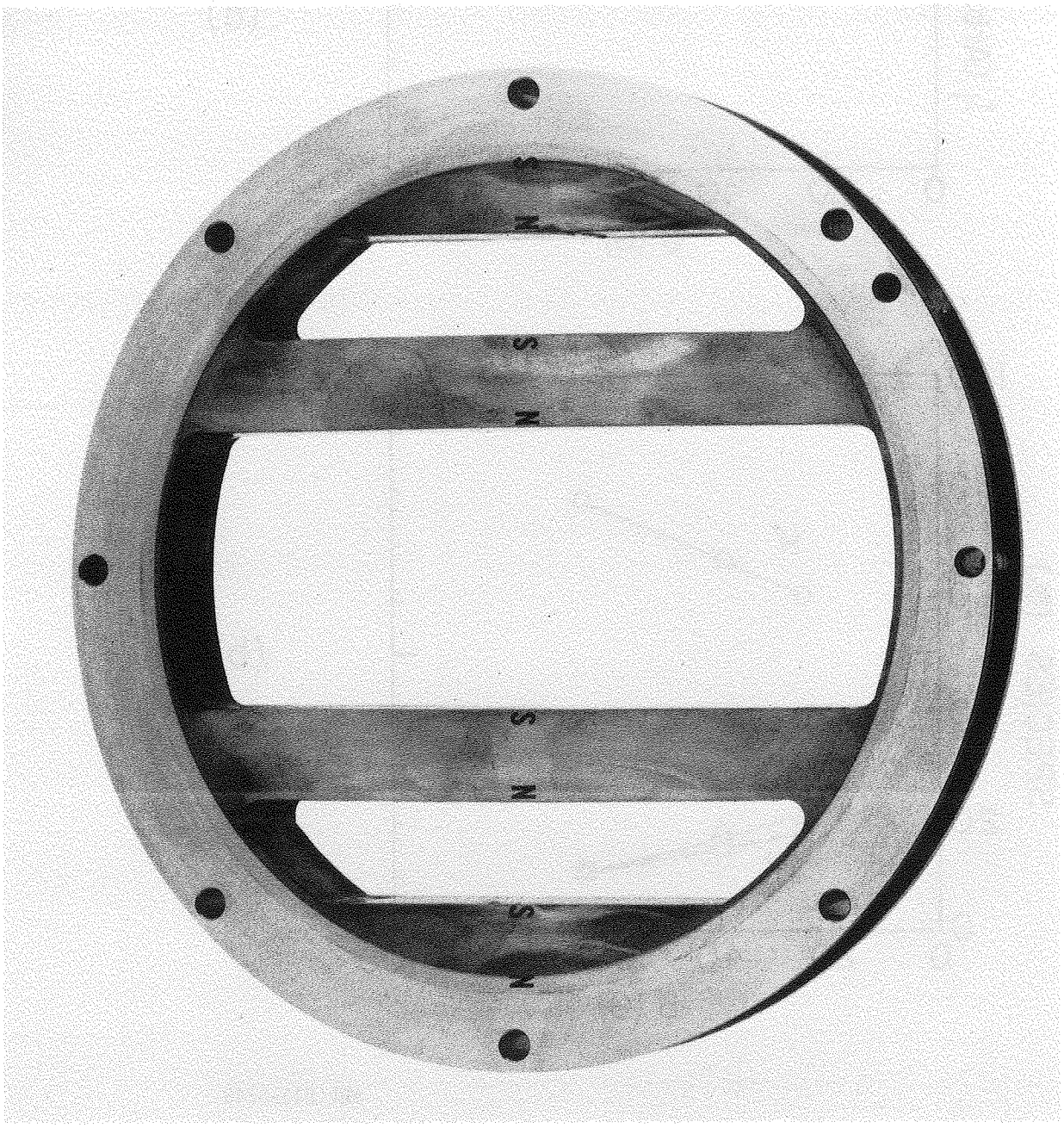

Fig. 8 CBB 811-535

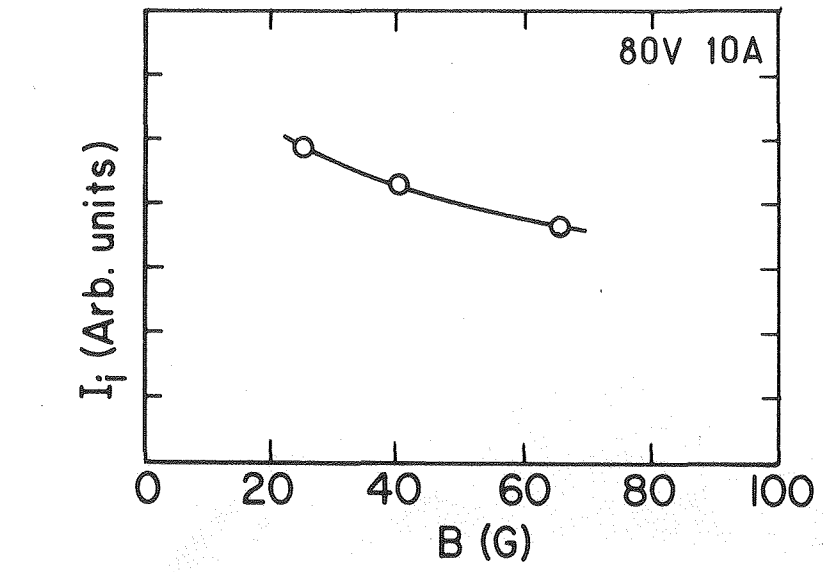

(a)

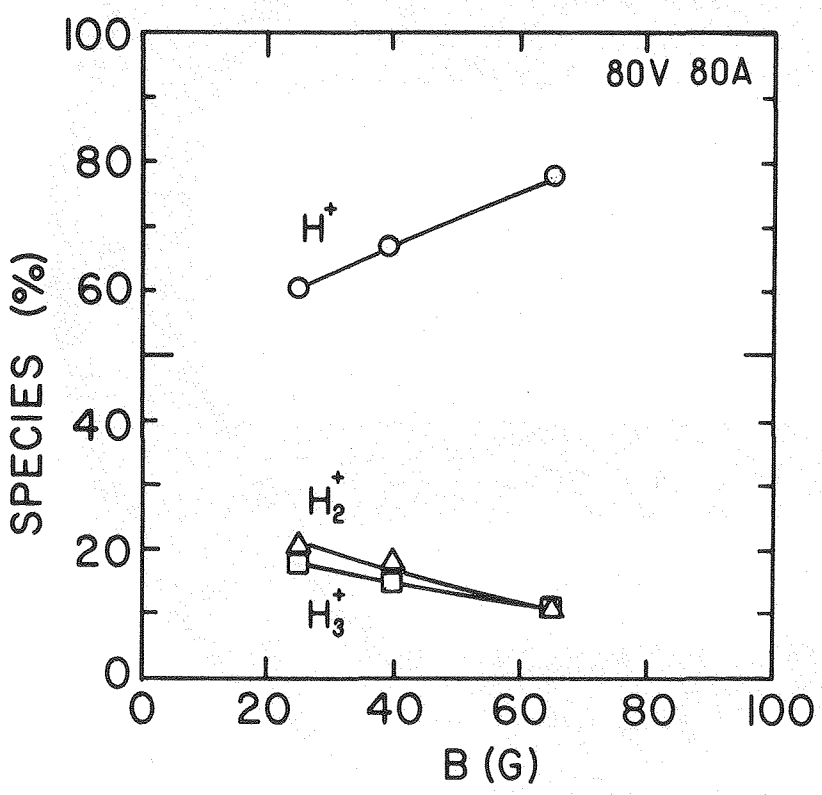

(b)

XBL 813-8748

Fig. 9

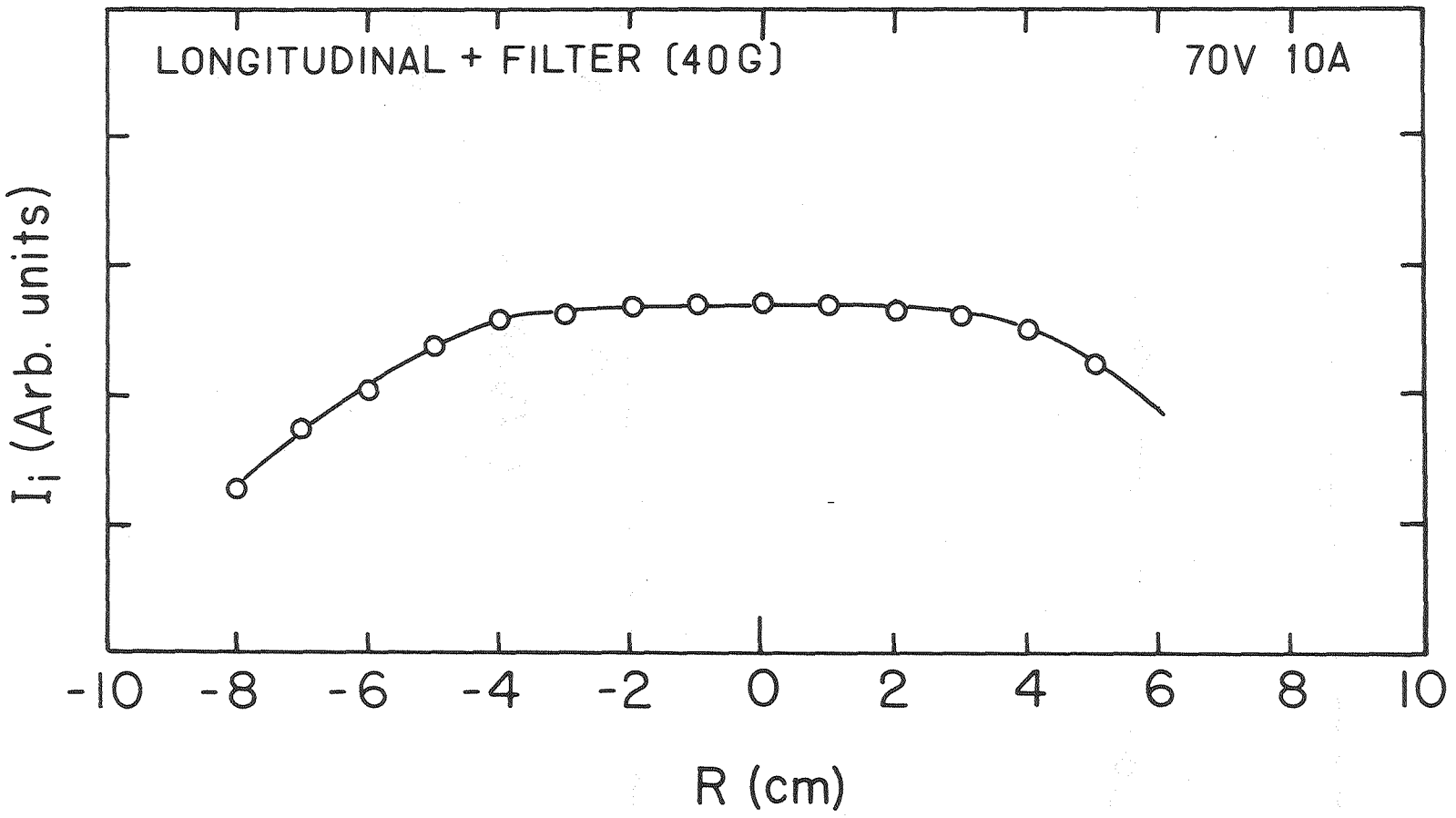

XBL 813-8742

Fig. 10

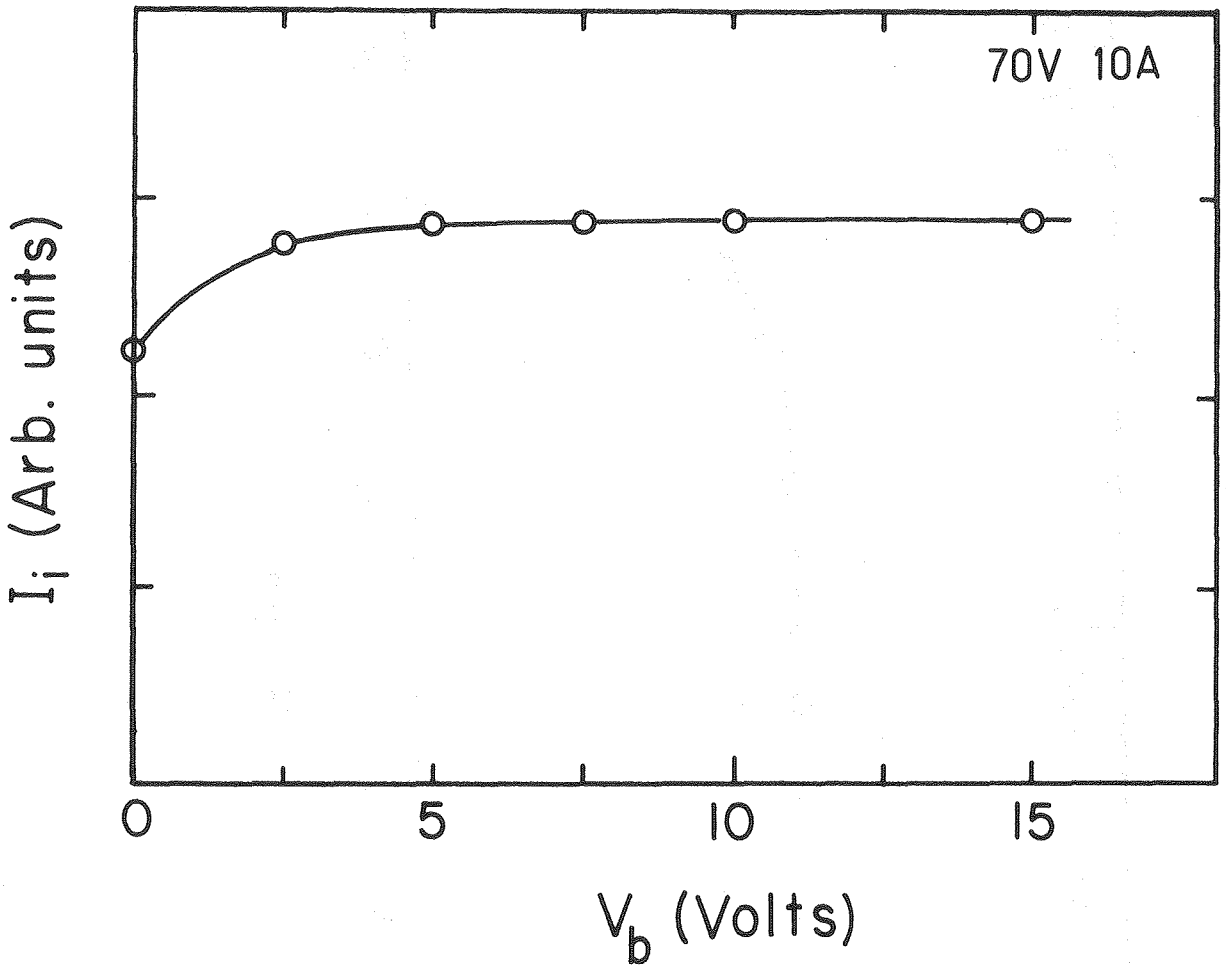

XBL 813-8755

Fig. 11

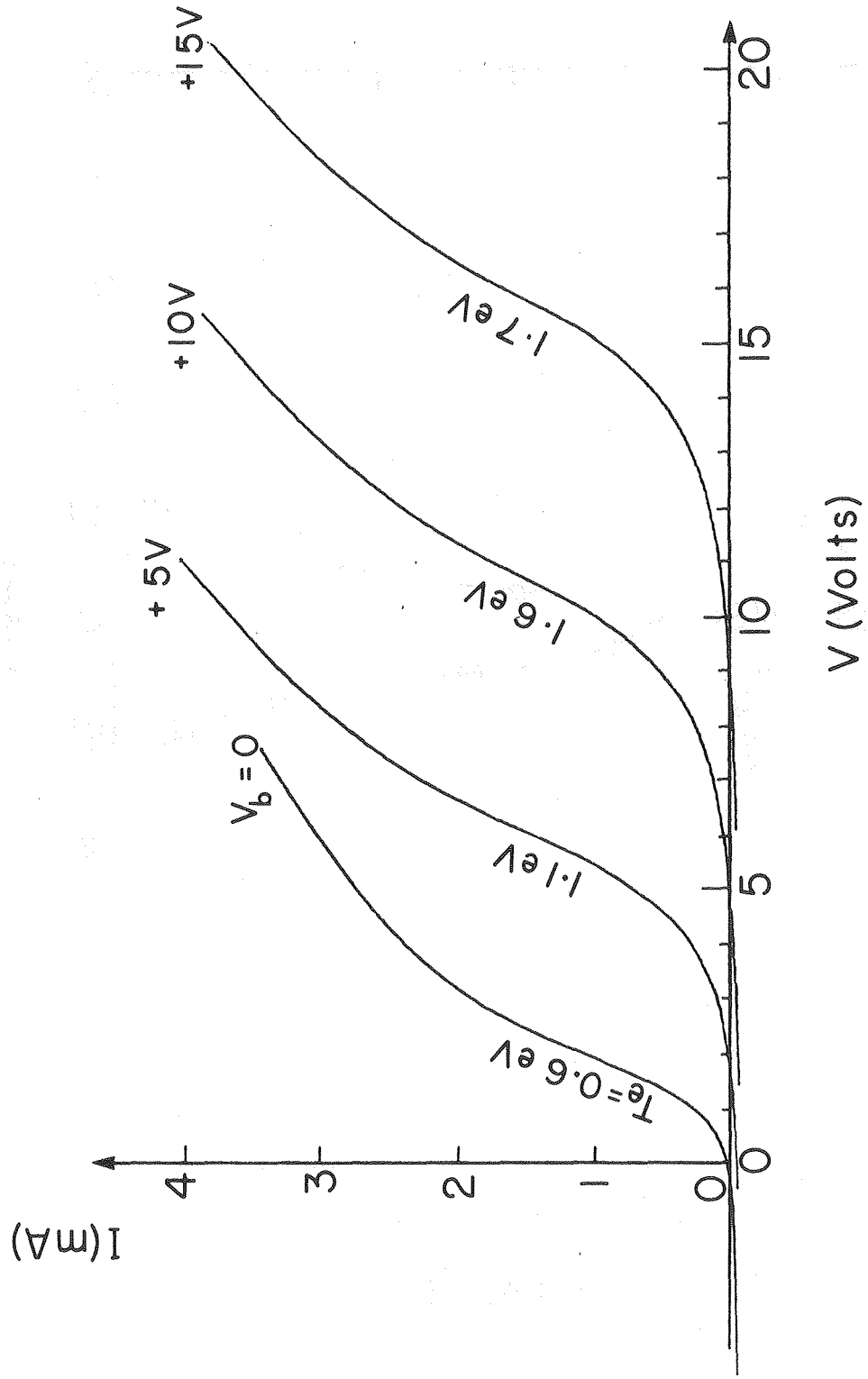

XBL 813-8744

Fig. 12

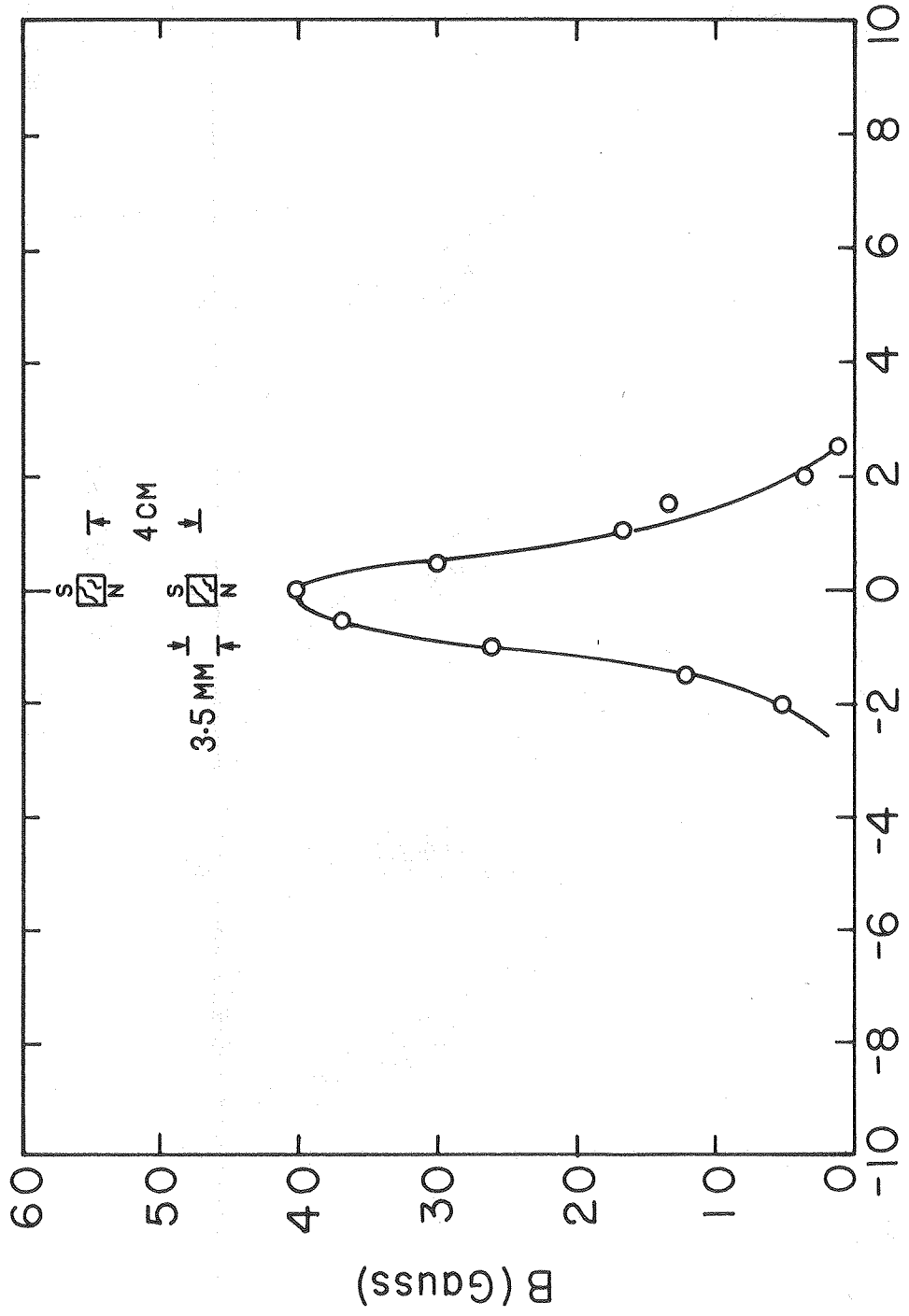

XBL 814-9142

Fig. 13

Ti (ARD. UIIIIS)

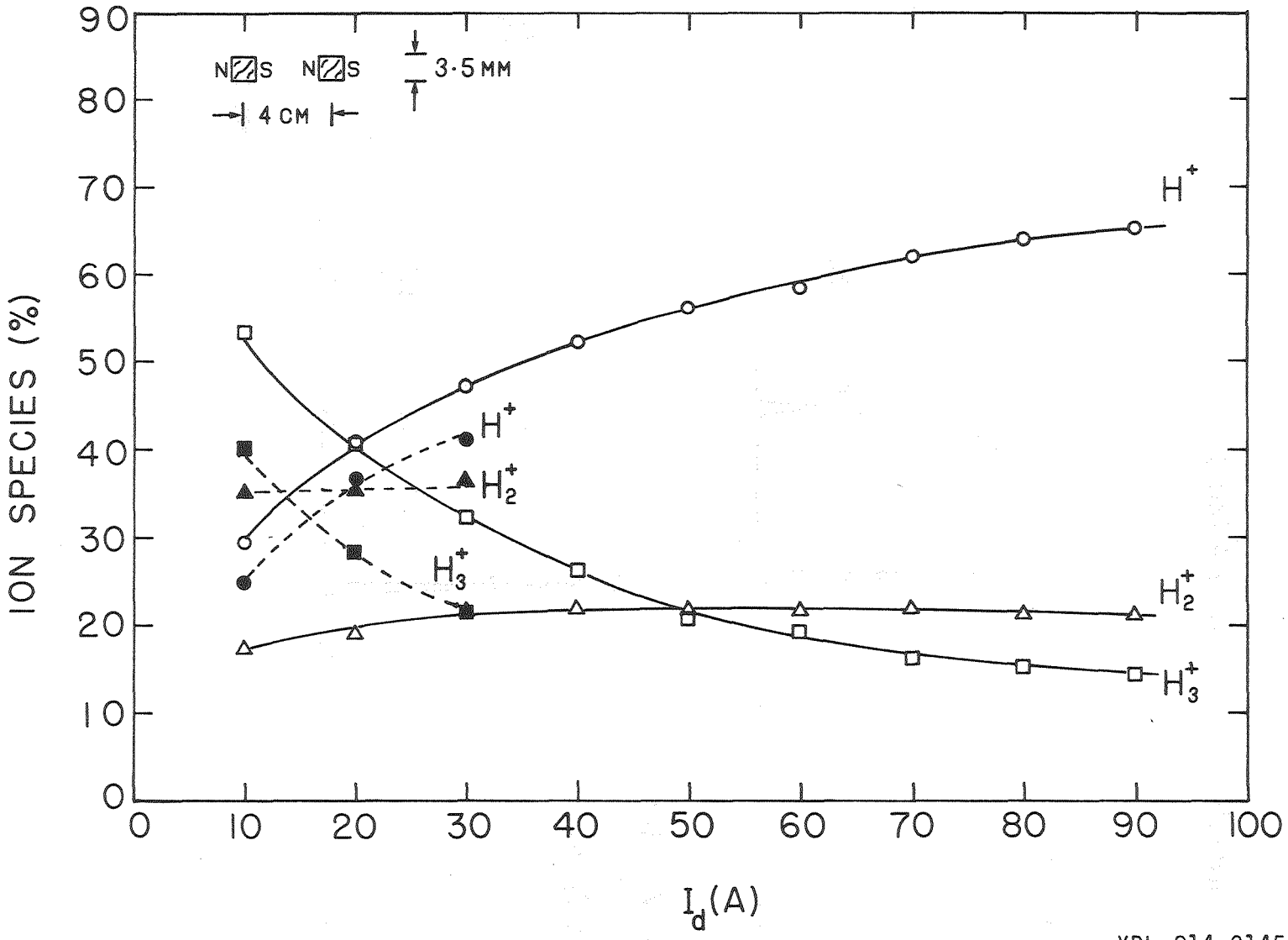

XBL 814-9145

Fig. 14

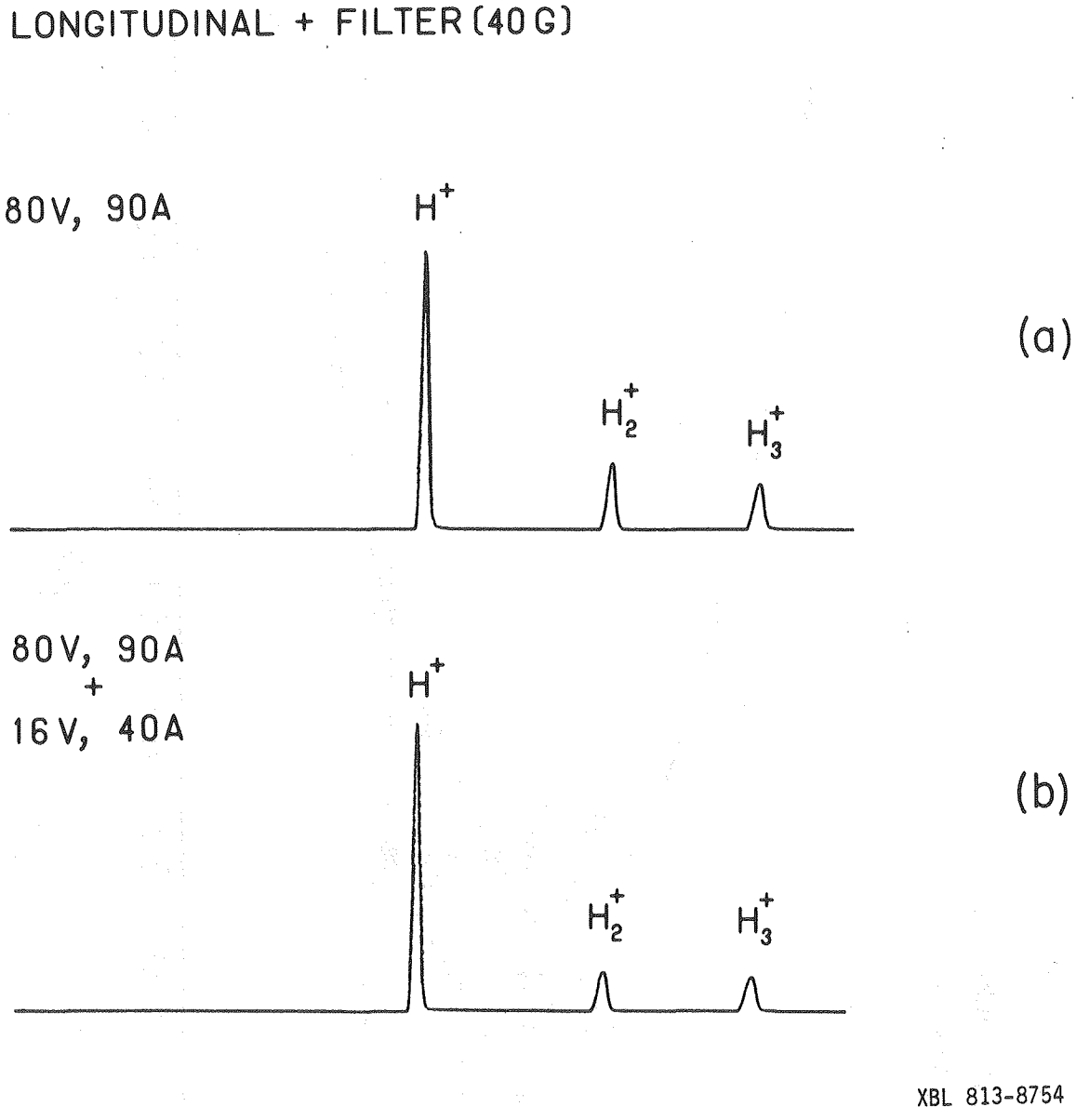
LONGITUDINAL + FILTER (40 G)
80V, 90A
H+
H2+
H3+
(a)
80V, 90A
+
16V, 40A
H+
H2+
H3+
(b)
XBL 813-8754

Fig. 15